

Title	Adsorption behavior of antimicrobial peptide histatin 5 on PMMA
Author(s) Alternative	Yoshinari, M; Kato, T; Matsuzaka, K; Hayakawa, T; Inoue, T; Oda, Y; Okuda, K; Shimono, M
Journal	Journal of biomedical materials research. Part B, Applied biomaterials, 77(1): 47-54
URL	http://hdl.handle.net/10130/64
Right	This is a preprint of an article published in Yoshinari M, Kato T, Matsuzaka K, Hayakawa T, Inoue T, Oda Y, Okuda K, Shimono M. Adsorption behavior of antimicrobial peptide histatin 5 on PMMA. J Biomed Mater Res B Appl Biomater. 2006 Apr;77(1):47-54.

b-05-0030

Adsorption Behavior of Antimicrobial Peptide Histatin 5 on PMMA

Masao Yoshinari¹, Tetsuo Kato², Kenichi Matsuzaka³, Tohru Hayakawa⁴, Takashi Inoue³,
Yutaka Oda¹, Katsuji Okuda², Masaki Shimono⁵

¹ Department of Dental Materials Science and Oral Health Science Center, Tokyo Dental College, 1-2-2 Masago, Mihama-ku, Chiba 261-8502, Japan

² Department of Microbiology and Oral Health Science Center, Tokyo Dental College, 1-2-2 Masago, Mihama-ku, Chiba 261-8502, Japan

³ Department of Clinical Pathophysiology and Oral Health Science Center, Tokyo Dental College, 1-2-2 Masago, Mihama-ku, Chiba 261-8502, Japan

⁴ Department of Dental Biomaterials, Research Institute of Oral Science, Nihon University School of Dentistry at Matsudo, 2-870-1, Sakaecho-nishi, Matsudo, Chiba 271-8587, Japan

⁵ Department of Pathology and Oral Health Science Center, Tokyo Dental College, 1-2-2 Masago, Mihama-ku, Chiba 261-8502, Japan

Correspondence to: Masao Yoshinari, Department of Dental Materials Science and Oral Health Science Center, Tokyo Dental College, 1-2-2 Masago, Mihama-ku, Chiba 261-8502, Japan
(e-mail: yosinari@tdc.ac.jp)

Running Heads: ADSORPTION of HISTATIN 5 on PMMA

Abstract: Adsorption of antimicrobial peptide histatin 5 on a poly(methyl methacrylate) denture base may serve to prevent biofilm formation, leading to a reduction of denture-induced stomatitis. This study focused on adsorption behavior of histatin 5 onto PMMA surfaces modified using a cold plasma technique and the effectiveness of histatin 5 adsorption for reducing *C. albicans* biofilm formation by the quartz crystal microbalance-dissipation (QCM-D) technique. PMMA spin-coated specimens were treated with oxygen (O₂) plasma using a plasma surface modification apparatus. The amount of histatin 5 adsorbed onto the PMMA treated with O₂ plasma is more than six times greater than that adsorbed onto untreated PMMA. The degree of histatin 5 adsorption had a negative correlation with the contact angle, whereas that of zeta-potential showed no significant correlation. XPS analysis revealed that the introduction of the carboxyl and O₂ functional groups were observable on the O₂ plasma treated PMMA. Increased surface hydrophilicity and the formation of the carboxyl could be responsible for histatin 5 adsorption on plasma-treated PMMA. There is no significant difference between histatin-adsorbed PMMA and control PMMA for *C. albicans* initially attached. On the contrary, the amount of *C. albicans* colonization on histatin-adsorbed PMMA was significantly less than the control.

Keywords:

antimicrobial, surface modification, glow discharge (RF/Plasma), histatin 5, PMMA

INTRODUCTION

Denture-induced stomatitis is a common intraoral disease, which is associated with high levels of *Candida albicans* (*C. albicans*) adhesion and biofilm formation to a poly(methyl methacrylate) (PMMA) denture base^{1,2,3}. *Candida* biofilms on PMMA were mostly blastophores with very few hyphal forms. Above the layer of cells, profuse matrix was seen which consisted of extracellular matrix and hyphal elements⁴. Biofilm cells are reported to be more resistant to antimicrobial agents compared with the planktonic cells⁵. For that reason, various surface modifications of PMMA surfaces, such as changes in the physicochemical nature^{6,7}, treatment with antibiotics^{8,9}, and antifungal agents¹⁰ have been attempted to reduce the adhesion of *C. albicans* on the denture surface.

The loading of antimicrobial peptides onto a PMMA denture is an important candidate for incorporating antimicrobial activity. Antimicrobial peptides are a new class of promising antimicrobial agents with a low tendency to induce resistance *in vitro*^{11,12}. This type of peptide is expected to be used in place of antibiotics because there are no known antibiotic-resistant bacteria such as methicillin-resistant *S. aureus* (MRSA) and there are no known side-effects.^{13,14} Clinical applications for antimicrobial peptides are currently under investigation, such as the saliva substitute xanthan loaded with antimicrobial peptides for treating oral candidosis¹⁵. Histatins, a family of basic peptides secreted by the major salivary glands in humans, possess antimicrobial activities. The antimicrobial activities are thought to be one means of regulating biofilm formation in the oral cavity¹⁶. Especially, histatin 5 is effective for its antimicrobial activity, and has fungicidal and fungistatic effects on *C. albicans* cells^{15,16}. Though some antimicrobial peptides have some side effects such as hemolysis, histatins showed no or low hemolytic activity using human erythrocytes^{17,18}. Consequently, surface loading of histatin 5 by either adsorption or chemical crosslinking provides a higher concentration of active molecules on the PMMA denture, leading to the reduction of *C.*

albicans biofilm formation. Edgerton M *et al.* showed that modification of PMMA at the surface by copolymerization of methyl methacrylic acid for introducing carboxyl groups resulted in a polymer that was capable of double the adsorption of the added amount of histatin 5 per surface area¹⁶.

Cold plasma surface modification using various gases such as Ar, O₂, N₂, and SO₂ has been utilized to modify blood compatibility, to influence cell adhesion and growth, and to control protein adsorption¹⁹⁻²². Notably, O₂ plasma treatment was reported able to control hydrophilicity/hydrophobicity and to introduce several functional groups leading to applications such as humidity sensors, enzyme immobilization, and polymer bonding without the use of adhesive²³⁻²⁵. Our previous study showed that the O₂ plasma treatment enabled introduction of an O₂ functional group on the surface and promoted the adhesion of proteins such as fibronectin on a hexamethyldisiloxane polymer²⁶.

Therefore, this study focused on modifying the PMMA surface via cold plasma treatment in order to provide functional groups to which histatin 5 would be adsorbed. Additionally, the effectiveness of histatin 5 surface adsorption was evaluated for reducing *C. albicans* biofilm formation by the quartz crystal microbalance-dissipation technique, which is useful for evaluating protein adsorption.

MATERIALS AND METHODS

Cold Plasma Treatment

PMMA-coated specimens were prepared on various substrates using a spin-coating system. As substrates for spin coating, coverslips (f=13 mm, Nunc, Tokyo, Japan) were used for surface roughness measurement, contact angle measurement, zeta-potential measurement, XPS analysis, and SEM observation. CaF₂ crystals (f=20 mm, JASCO, Tokyo, Japan) were used for FT-IR analysis. QCM sensors (f=14 mm, Q-Sense AB, Göteborg, Sweden) were used for the

adsorption assay of histatin 5, and initial attachment and colonization assay of *C. albicans*. The PMMA polymer (Wako, Osaka, Japan) has a molecular weight of 80,000 and a density of 1.19-1.20g/cm³ at 25°C. The polymer films were dissolved in a chloroform solution (mass fraction of 4%). The solution was spin coated onto various substrates at 4000 rpm for 20 s using a spin coater (1H-D7, Mikasa, Tokyo, Japan). The films were then dried under vacuum for 24 h and were stored in a desiccator at room temperature. The film thickness under these conditions was approximately 200 nm as determined by a QCM-D instrument (QCM-D300, Q-Sense AB, Göteborg, Sweden) that was mentioned in “Adsorption Assay of Histatin 5”. Briefly, a frequency shift of spin-coated PMMA showed about 10,000 Hz was converted into the mass of 2.53 x 10,000 ng/cm², and then the mass was divided by a density of PMMA of 1.20g/cm³ and was finally converted into film thickness of ~ 200 nm.

PMMA-coated specimens were treated with O₂ for 10 min at room temperature with a gas flow rate of 50 sccm (mL/min) and a chamber pressure of 1.5 Pa using a commercially available plasma surface modification apparatus (VEP-1000, ULVAC Inc., Kanagawa, Japan). The plasma was generated using a radiofrequency generator operating at 13.56 MHz at a power level of 200 W. Finally, as-spin-coated PMMA (PMMA) and O₂ plasma treated (PMMA-O₂) were prepared.

Surface Characterization of Cold Plasma-treated Surfaces

The surface roughness of the PMMA and the PMMA-O₂ were measured by a Handy Surf E-30A (Tokyo Seimitsu, Tokyo, Japan). Measurement was done on 3 randomly selected fields of each sample and the mean surface roughness (Ra) was calculated.

The contact angle with respect to double-distilled water was measured using a Contact Angle Meter (CA-P, Kyowa Interface Science Co. Ltd., Tokyo, Japan). Five measurements of 15 s each were made for each surface type; all analyses were performed at the same temperature and

humidity.

The zeta-potential of the surfaces were measured using an electrophoretic light scattering spectrophotometer (ELS-6000, Ohtsuka Electronics, Tokyo, Japan). Measurements were performed in 10 mM NaCl solution at 25°C using latex particles as a monitor in the cell for flat plate sample. Data presented are the mean of measurements of three samples, each of which were measured four times.

An X-ray photoelectron spectroscopy (XPS) analysis (ESCA-750, Shimadzu, Kyoto, Japan) was performed with Mg-K α as an X-ray source at 8 kV and 30 mA for measuring the intensity of C1s and O1s. The binding energy of each spectrum was calibrated with C1s of 285.0 eV for charging correction. Resolution of the instrument was 1.15 eV of FWHM at Ag 3d 5/2. Baseline correction was done with a conventional Shirley method, and peak fitting and deconvolution were performed with reference to the database²⁷. Fourier transform infrared absorption spectroscopy (FT-IR-430, Jasco Corp., Tokyo, Japan) analysis was conducted with PMMA spin coated on CaF₂ crystals at a resolution of 4-cm⁻¹. Each surface type was measured three times.

Adsorption Assay of Histatin 5

Schematic illustrations of PMMA spin coating, plasma treatment, and adsorption assay for QCM-D measurement are shown in Figure 1.

Commercially available histatin 5 (Asp-Ser-His-Ala-Lys-Arg-His-His-Gly-Tyr-Lys-Arg-Lys-Phe-His-Glu-Lys-His-His-Ser-His-Arg-Gly-Tyr, Human, 4270-S, Peptide Institute, Japan) and QCM-D instrument as mentioned above were used for the adsorption assay. The QCM-D instrument was operated with AT-cut single-crystal quartz sensors with a resonant frequency of 5 MHz for the adsorption assay. The crystal resonant frequency (f) and the dissipation factor (D) of the oscillator were measured simultaneously at a fundamental resonant frequency (5 MHz) and at a number of overtones,

including 35 MHz. Monitoring the resonance behavior of piezoelectric oscillation enables measurements of mass adsorption at the surface in real time, usually as a function of the decrease in resonance frequency. The frequency shift is related to the adsorbed mass; the adsorbed mass was estimated by the Sauerbrey equation²⁸. The adsorbed mass is calculated by the following equation as a function of frequency change (Δf).

$$\Delta m = (-C \Delta f) / n$$

Here $C = 17.7 \text{ ng Hz}^{-1} \text{ cm}^{-2}$ for a 5 MHz quartz crystal, $n = 1,3,5,7$ is the overtone number.

At 35 MHz, a frequency shift of 1 Hz corresponds to a mass change of approximately 2.53 ng/cm^2 .

A second measurement parameter, dissipation (D), gives qualitative information about the viscoelastic properties of the adsorbed layer. The increase in energy dissipation is proportional to the root of the product of viscosity and density. If the adsorbed layer is rigid, a low ΔD value would be obtained.

A histatin 5 solution in PBS (-) ($10 \mu\text{g/mL}$, $\text{pH} = 7.4$) was introduced into an axial flow chamber consisting of a T-loop in order to thermally equilibrate the sample at $25 \pm 0.05^\circ\text{C}$. The sequence of injections into the QCM cell for an experimental run was as follows: 0.5 mL of PBS (-), 0.5 mL of histatin 5 solution, and 0.5 mL of PBS (-). The results were expressed as the mean \pm SD of five specimens..

Initial Attachment and Colonization Assay against *C. albicans*

The initial attachment and colonization assay against *C. albicans* JCM 1542 (Riken, Saitama, Japan) was performed using the QCM-D instrument as mentioned above. PMMA spin coated (PMMA) as a control, PMMA-O₂ and histatin-adsorbed specimens (PMMA-O₂-His) were evaluated. Adsorption of histatin 5 was accomplished with the following steps: treatment with O₂ plasma for 10 min, immersion in 0.5 mL of histatin 5 solution in PBS (-) ($10 \mu\text{g/mL}$, $\text{pH} =$

7.4) for 2 hours at room temperature, and gentle washing with distilled water. A *C. albicans* strain was cultured in broth (glucose 10 g, peptone 5 g, and yeast extract 3g/ 1L water) at room temperature for one day. A 0.3-mL sample including approximately 10^6 /mL of *C. albicans* strain was directly introduced into the window chamber of the QCM-D instrument. After incubation for one day, the culture medium that included unattached cells was removed by the use of a micropipette and washed two times with culture medium. At this point, the crystal resonant frequency (Δf) was measured as the amount of initial attachment of *C. albicans*. After that the measurement, 0.3 mL of the culture medium was added into the window chamber and *C. albicans* were cultured for one day. At this point, Δf was measured as the amount of colonized *C. albicans* as a biofilm formation. The results were expressed as the mean \pm SD of three specimens.

Scanning Electron Microscopy

PMMA-coated coverslips were incubated with *C. albicans* in the same way as for the biofilm formation assay. The specimens were fixed in 1.0% glutaraldehyde in PBS (-) solution for 2 hours at room temperature, and then washed 3 times with PBS (-) solution and dehydrated through a series of graded ethanol solutions (70%, 80%, 90%, 95%, and 100%). The specimens were subsequently freeze-dried, sputter-coated with Au-Pd, and observed using a scanning electron microscope (JSM-6340F, JEOL, Japan).

Statistical Analysis

The data was analyzed for statistical significance using analysis of variance (ANOVA) followed by Scheffe's test for multiple comparisons.

RESULTS

Surface Characterization after Cold Plasma Treatment

Both control PMMA and the PMMA-O2 showed mirror-like surfaces with $0.06 \pm 0.01 \mu\text{m}$ and $0.07 \pm 0.02 \mu\text{m}$ of Ra, respectively, and there was no significant difference in Ra between specimens ($p > 0.05$).

The contact angles were 68 ± 4 degrees on the PMMA. These values decreased dramatically after the O₂ plasma treatment (PMMA-O2) with 14 ± 2 degrees ($p < 0.01$).

The zeta-potentials were -38 ± 5 mV on the PMMA and -28 ± 7 mV on the PMMA-O2 surfaces, respectively, that were comparable with reported values²⁹. There was no significant differences between the specimens ($p > 0.05$).

The XPS spectra of the PMMA and PMMA-O2 specimens are shown in Figure 2. To identify the molecular species present in the C1s and O1s spectra, Gaussian model peaks were fitted in the spectra. In the C1s peak of the PMMA surface, C-H (C-C), C-OH (C-O), and C=O peaks appeared at around 285.0 eV, 286.6 eV, and 288.6 eV, which corresponded to C-CH_x, the carbonyl group, and the carboxyl group, respectively. The C=O peak increased on the PMMA-O2 specimen in comparison to the PMMA specimen. In the O1s peak, OH and C=O peaks appeared at around 532.6 eV and 534.2 eV, respectively. The intensity ratios of the O/C element and carboxyl group to the CH_x group (C=O/C-H) on the PMMA and PMMA-O2 surfaces are shown in Figure 3. Compared to that of the PMMA specimen, the intensity of O was increased on the PMMA-O2 specimen ($p < 0.01$). The intensity ratio of C=O/C-H became higher in the sequence, PMMA-O2 > PMMA ($p < 0.01$).

The FT-IR spectra of the PMMA and PMMA-O2 specimens are shown in Figure 4. All spectra were identified as polymethylmethacrylate (BP #1455) by the Sadtler search system. No apparent changes were observable between the specimens.

Adsorption of Histatin 5

Figure 5 (a) shows Δf and ΔD versus time and (b) the ΔD - Δf plot of histatin 5 adsorption on the PMMA-O2 specimen as a schematic example. The break point was observed in the ΔD - Δf plot, indicating change in rigidity and density of adsorbed histatin 5 before and after the break point.

The estimated amounts of histatin 5 adsorption on the QCM sensors are shown in Figure 6 with the measurement results of contact angle and zeta-potential. The amount of histatin 5 adsorption was estimated by the Sauerbrey equation²⁸ 1 h after injection of the histatin 5 solution. The amount of histatin 5 adsorption onto the PMMA-O2 sensors was more than six times greater than that onto the PMMA sensor ($p < 0.01$). The amounts of histatin 5 adsorption showed a significant negative correlation with the contact angle, whereas that of the zeta-potential showed no significant correlation.

Initial Attachment and Colonization of *C. albicans*

Figure 7(a) plots a typical example of the shift in frequency and dissipation versus time for exposure of the PMMA specimen to *C. albicans* as obtained via QCM-D measurement. The SEM images are also shown in Figure 7(a). The starting point (1) of this graph is after one day of incubation, i.e., after the initial attachment of *C. albicans*. The frequency curve shows a decrease over time during the early stages of attachment until it reached a certain frequency after about 10 hrs. Fungal attachment was observed on the substrates at the initial stage (1) of SEM observation. Hyphae formation was observed after 3 hrs of incubation (2), and fungal colonization proceeded after 8 hrs of incubation (3). At 22 hrs of incubation (4), the *C. albicans* cells observed embedded in the extracellular polymeric material had an amorphous granular appearance³⁰. A dissipation shift (ΔD) was observed to be almost the reverse tendency to the frequency shift. The ΔD - Δf plot for exposure of the PMMA specimen to *C. albicans* is shown in Figure 7(b) as a schematic example. The break point was observed in the ΔD - Δf plot (at ~ 2 hrs),

showing change in rigidity of fungal attachment before and after the break point during the colonization of *C. albicans*.

The amounts of *C. albicans* initially attached (one day of incubation) and colonized (one day of incubation after initial attachment) are shown in Figure 8. There was no significant difference in the amount of initial attachment at point (1) of *C. albicans* among the specimens ($p>0.05$). However, there was a significant difference in the amount of *C. albicans* fungal colonization at point (4) between specimens with and without histatin-5 adsorption ($p<0.01$).

DISCUSSION

The purpose of the present study was to evaluate the adsorption behavior of histatin 5 onto plasma surface modified PMMA by using the quartz crystal microbalance-dissipation (QCM-D) technique as well as surface characterization. This study also determined the effectiveness of histatin 5 adsorption for reducing *C. albicans* biofilm formation.

Recent studies have confirmed that the quartz crystal microbalance-dissipation (QCM-D) technique is useful for evaluating surface-related processes with a real-time measurement in liquids, including protein adsorption, complementary activity on biomaterials, and analysis of DNA hybridization³¹⁻³⁶. Höök et al. reported the effectiveness of the QCM-D technique for analyzing the adsorption kinetics of three model proteins on titanium oxide surfaces compared with ellipsometry and optical waveguide lightmode spectroscopy³⁴. QCM-D measurement was performed to obtain more detailed information about the quantity of protein adsorption, and the QCM system offered advantages of short response times compared to conventional immunoassay systems³⁶. They also pointed out that the mass calculated from the resonance frequency shift included both protein mass and water that was bound or hydrodynamically coupled to the protein adlayer. The results in this study showed a clear difference of frequency shift among the conditions on both the histatin adsorption assay and the colonization assay of

the *C. albicans*. These results indicate that the QCM-D technique is effective in the evaluation of the adsorption behavior of peptides such as histatin 5 and the biofilm formation behavior of fungi with comparatively high molecular weights.

The ΔD (dissipation factor) - Δf (frequency factor) plot of histatin 5 adsorption in Figure 5 (b) showed the break point in the plot. This phenomenon demonstrates that the frequency change after the first adsorption process (before the break point in the ΔD - Δf plot) was consistent with the approximate formation of a monolayer. In contrast, after the second process (at ~ 5 min), the slope of the ΔD - Δf plot becomes steep, indicating formation of a multilayer³⁷. The break point of ΔD - Δf plot for exposure of the PMMA specimen to *C. albicans* was also observed in Figure 7(b) at around 2 hrs, suggesting the shift from fungal attachment to hyphae formation.

This study showed that the change in surface functional groups in the experimentally modified PMMA polymer permitted superior adsorption properties for histatin 5. The amount of histatin 5 adsorption onto O_2 treated sensor coated with PMMA was more than six times greater than that onto sensors without modification. The amount of histatin 5 adsorption had a negative correlation with the contact angle, whereas that of zeta-potential showed no significant correlation. In addition, XPS analysis revealed that the introduction of the carboxyl group and O_2 -functional group onto the PMMA surface by O_2 plasma treatment. On FT-IR analysis, all spectra were identified as polymethylmethacrylate, but no apparent changes were observed among the specimens. This is due to the ultra-thin modified layers compared to thickness of spin-coated PMMA.

Histatin 5 molecules have cationic ions ($pI > 9$, positively charged at $pH = 7.4$) and are amphipathic with both hydrophilic and hydrophobic domains³⁸. Therefore, it was expected that histatin 5 would easily be absorbed on the untreated PMMA that was negatively charged (zeta potential = -38 mV) through electrostatic force. However, small amounts of histatin 5 were

absorbed on PMMA surface compared to those on O₂ plasma treated PMMA surfaces. Accordingly, it is considered that there are two possible explanations for increasing the histatin 5 adsorption by O₂ plasma treatment. On one hand, the increase of surface energy by plasma treatment increases the van der Waals force. On the other hand, the hydrogen bond mediated by the carboxyl group for the PMMA-O₂ specimens could be responsible for this mechanism^{16, 39}. Further investigation should be performed to clarify bonding mechanism more accurately.

There is no significant difference in the amount of initial attachment of *C. albicans* among the control (PMMA), O₂-treated PMMA and the histatin-adsorbed PMMA. However, the amount of *C. albicans* biofilm formation on the histatin-adsorbed PMMA significantly decreased compared to that on the other specimens. These results indicate that histatin-adsorption does not prevent or reduce adhesion of the microorganism to the denture surface, but that direct candidacidal activity of the adsorbed molecules is responsible for reducing *C. albicans* biofilm formation on the denture surface. In addition, the facts that O₂-treated PMMA did not reduce the biofilm formation proved that the reduction of fungal growth was attributed to the histatin 5 and not the change in surface properties of PMMA.

In summary, histatin 5 adsorption increased onto PMMA by oxygen plasma treatment, and *C. albicans* colonization on PMMA was decreased significantly by histatin 5 adsorption. In addition, increasing surface hydrophilicity and the formation of a carboxyl group could be responsible for histatin 5 adsorption on plasma-treated PMMA. The limitations of this study are that the temperature was not physiological and the stability of adsorbed histatin 5 was not evaluated under oral environment. However, this study mainly focused on the adsorption behavior of histatin 5 onto PMMA using plasma treatment under controlled conditions⁴⁰. Further study is necessary to investigate the stability of adsorbed histatins by exposing to simulated saliva, and to establish the method for direct loading of histatins from saliva in oral environment.

ACKNOWLEDGMENTS

This study was supported by the Oral Health Science Center Grant 5A10 from Tokyo Dental College, by “High-Tech Research Center” Project for Private Universities : matching fund subsidy from MEXT (Ministry of Education, Culture, Sports, Science and Technology) of Japan,2001-2005, by a Grant-in-Aid for Scientific Research (C)(2) (15592065) from the Japan Society for the Promotion of Science, and by a grant from MEXT of Japan to promote 2001-Multidisciplinary Research Projects (2001- 2005).

REFERENCES

1. Gocke R, Gerath F, von Schwanewede H. Quantitative determination of salivary components in the pellicle on PMMA denture base material. *Clin Oral Investig* 2002;6:227-235.
2. Costerton JW, Lewandowski Z, Caldwell DE, Korber DR, Lappin-Scott HM. Microbial biofilms. *Annu Rev Microbiol* 1995;49:711-745.
3. Budtz-Jorgensen E, Stenderup A, Grabowski M. An epidemiologic study of yeasts in elderly denture wearers. *Community Dent Oral Epidemiol* 1975; 3: 115-119.
4. Chandra J, Kuhn DM, Mukherjee PK, Hoyer LL, McCormick T, Ghannoum MA. Biofilm formation by the fungal pathogen *Candida albicans*: development, architecture, and drug resistance. *J Bacteriol* 2001;183:5385-5394.
5. Chandra J, Mukherjee PK, Leidich SD, Faddoul FF, Hoyer LL, Douglas LJ, Ghannoum MA. Antifungal resistance of candidal biofilms formed on denture acrylic in vitro. *J Dent Res* 2001;80:903-908.
6. Park SE, Periathamby AR, Loza JC. Effect of surface-charged poly(methyl methacrylate) on the adhesion of *Candida albicans*. *J Prosthodont* 2003;12:249-254.
7. Waltimo T, Vallittu P, Haapasalo M. Adherence of *Candida* species to newly polymerized and water-stored denture base polymers. *Int J Prosthodont* 2001;14:457-460.
8. Weisman DL, Olmstead ML, Kowalski JJ. In vitro evaluation of antibiotic elution from polymethylmethacrylate (PMMA) and mechanical assessment of antibiotic-PMMA composites. *Vet Surg* 2000;29:245-251.
9. Anagnostakos K, Kelm J, Regitz T, Schmitt E, Jung W. In vitro evaluation of antibiotic release from and bacteria growth inhibition by antibiotic-loaded acrylic bone cement spacers. *J Biomed Mater Res* 2005;72B:373-378.

10. Lamfon H, Al-Karaawi Z, McCullough M, Porter SR, Pratten J. Composition of in vitro denture plaque biofilms and susceptibility to antifungals. *FEMS Microbiol Lett* 2005;242:345-351.
11. Hancock RE. Peptide antibiotics. *Lancet* 1997;349:418-422.
12. Zasloff M. Antimicrobial peptides of multicellular organisms. *Nature* 2002; 415:389-395.
13. Helmerhorst EJ, Hodgson R, van 't Hof W, Veerman EC, Allison C, Nieuw Amerongen AV. The effects of histatin-derived basic antimicrobial peptides on oral biofilms. *J Dent Res* 1999;78:1245-1250
14. Gusman H, Lendenmann U, Grogan J, Troxler RF, Oppenheim FG. Zn(2+) ions selectively induce antimicrobial salivary peptide histatin-5 to fuse negatively charged vesicles. Identification and characterization of a zinc-binding motif present in the functional domain. Is salivary histatin 5 a metalloprotein? *Biochim Biophys Acta* 2001;1545:86-95.
15. Ruissen AL, van der Reijden WA, van't Hof W, Veerman EC, Nieuw Amerongen AV. Evaluation of the use of xanthan as vehicle for cationic antifungal peptides. *J Control Release* 1999;60:49-56.
16. Edgerton M, Raj PA, Levine MJ. Surface-modified poly(methyl methacrylate) enhances adsorption and retains anticandidal activities of salivary histatin 5. *J Biomed Mater Res* 1995;29:1277-1286.
17. Wei GX, Bobek LA. In vitro synergic antifungal effect of MUC7 12-mer with histatin-5 12-mer or miconazole. *J Antimicrob Chemother* 2004;53:750-758.
18. Helmerhorst EJ, Reijnders IM, van 't Hof W, Veerman EC, Nieuw Amerongen AV. A critical comparison of the hemolytic and fungicidal activities of cationic antimicrobial peptides. *FEBS Lett* 1999; 449:105-110.
19. Suzuki M, Kishida A, Iwata H, Ikada Y. Graft copolymerization of acrylamide onto a

- polyethylene surface prepared with glow discharge. *Macromolecules* 1986;19: 1804-1808.
20. Bisson I, Kosinski M, Ruault S, Gupta B, Hilborn J, Wurm F, Frey P. Acrylic acid grafting and collagen immobilization on poly(ethylene terephthalate) surfaces for adherence and growth of human bladder smooth muscle cells. *Biomaterials* 2002;23:3149-3158.
 21. Ito K, Kondo S, Kuzuya M. A new drug delivery system using plasma-irradiated pharmaceutical aids IX. *Chem Pharm Bull* 2001;49:1615-1620.
 22. Ding Z, Chen J, Gao S, Chang J, Zhang J, Kang ET. Immobilization of chitosan onto poly-lactic acid film surface by plasma graft polymerization to control the morphology of fibroblast and liver cells. *Biomaterials* 2004;25:1059-1067.
 23. Suzuki T, Tanner P, Thiel DV. O₂ plasma treated polyimide-based humidity sensors. *Analyst* 2002;127:1342-1346.
 24. Ganapathy R, Sarmadi M, Denes F. Immobilization of alpha-chymotrypsin on oxygen RF-plasma functionalized PET and PP surfaces. *J Biomater Sci Polym Ed* 1998;9:389-404.
 25. Wu Z, Xanthopoulos N, Reymond F, Rossier JS, Girault HH. Polymer microchips bonded by O₂-plasma activation. *Electrophoresis* 2002;23:782-790.
 26. Yoshinari M, Hayakawa T, Matsuzaka K, Inoue T, Oda Y, Shimono M. Immobilization of fibronectin onto organic hexamethyldisiloxane coatings with plasma surface modification -Analysis of fibronectin adsorption using quartz crystal microbalance-dissipation technique-, *J Oral Tissue Eng* 2004;1:69-79.
 27. Beamson G, Briggs D. High resolution XPS of organic polymers: The Scienta ESCA300 Database. Chichester: John Wiley & Sons; 1992.
 28. Sauerbrey G. Verwendung von Schwingquarzen zur Wägung dünner Schichten und zur Mikrowägung. *Z Phys* 1959;155:206-222.

29. Kirby BJ, Hasselbrink Jr EF. Zeta potential of microfluidic substrates: 2. Data for polymers, *Electrophoresis* 2004;25:203–213.
30. Chandra J, Ghannoum MA. Fungal biofilms: Ghannoum M, O'Toole GA, editors. *Microbial biofilms*. Washington DC: ASM Press;2004;p30-42.
31. Miyachi H, Hiratsuka A, Ikebukuro K, Yano K, Muguruma H, Karube I. Application of polymer-embedded proteins to fabrication of DNA array. *Biotechnol Bioeng* 2000;69:323-329.
32. Puleo DA, Kissling RA, Sheu M-S. A technique to immobilize bioactive proteins, including bone morphogenetic protein-4 (BMP-4), on titanium alloy. *Biomaterials* 2002;23:2097-2087.
33. Rodahl M, Höök F, Kasemo B. QCM operation in liquids: An explanation of measured variations in frequency and Q factor with liquid conductivity. *Anal Chem* 1996;68:2219-2227.
34. Höök F, Vörös J, Rodahl M, Kurrat R, Böni P, Ramsden JJ, Textor M, Spencer ND, Tengvall P, Gold J, Kasemo B. A comparative study of protein adsorption on titanium oxide surface using in situ ellipsometry, optical waveguide lightmode spectroscopy, and quartz crystal microbalance/dissipation. *Colloids Surf B Biointerfaces* 2002;24:155-170.
35. Andersson A-S, Glasmästar K, Sutherland D, Lidberg Ulf, Kasemo B. Cell adhesion on supported lipid bilayers. *J Biomed Mater Res* 2003;64A:622-629.
36. Lin S, Lu CC, Chien HF, Hsu SM. An on-line quantitative immunoassay system based on a quartz crystal microbalance. *J Immunol Methods* 2000; 26; 121-124.
37. Höök F, Rodahl M, Kasemo B, Brzezinski P. Structural changes in hemoglobin during adsorption to solid surfaces: Effects of pH, ionic strength, and ligand binding. *Proc Natl Acad Sci USA* 1998; 95:12271-12276.
38. Amerongen AV, Veerman EC. Saliva-the defender of the oral cavity. *Oral Dis* 2002;8:12-22.
39. Kang IK, Kwon BK, Lee JH, Lee HB. Immobilization of proteins on poly(methyl methacrylate)

films. *Biomaterials* 1993;14:787-792.

40. Faber C, Stallmann HP, Lyaruu DM, de Blicck JM, Bervoets TJ, van Nieuw Amerongen A, Wuisman PI. Release of antimicrobial peptide Dhvar-5 from polymethylmethacrylate beads. *J Antimicrob Chemother* 2003;51:1359-1364.

Legend for figures

Figure 1 Schematic illustrations of (1) PMMA spin coating, (2) plasma treatment, and (3) adsorption assay for QCM-D measurement.

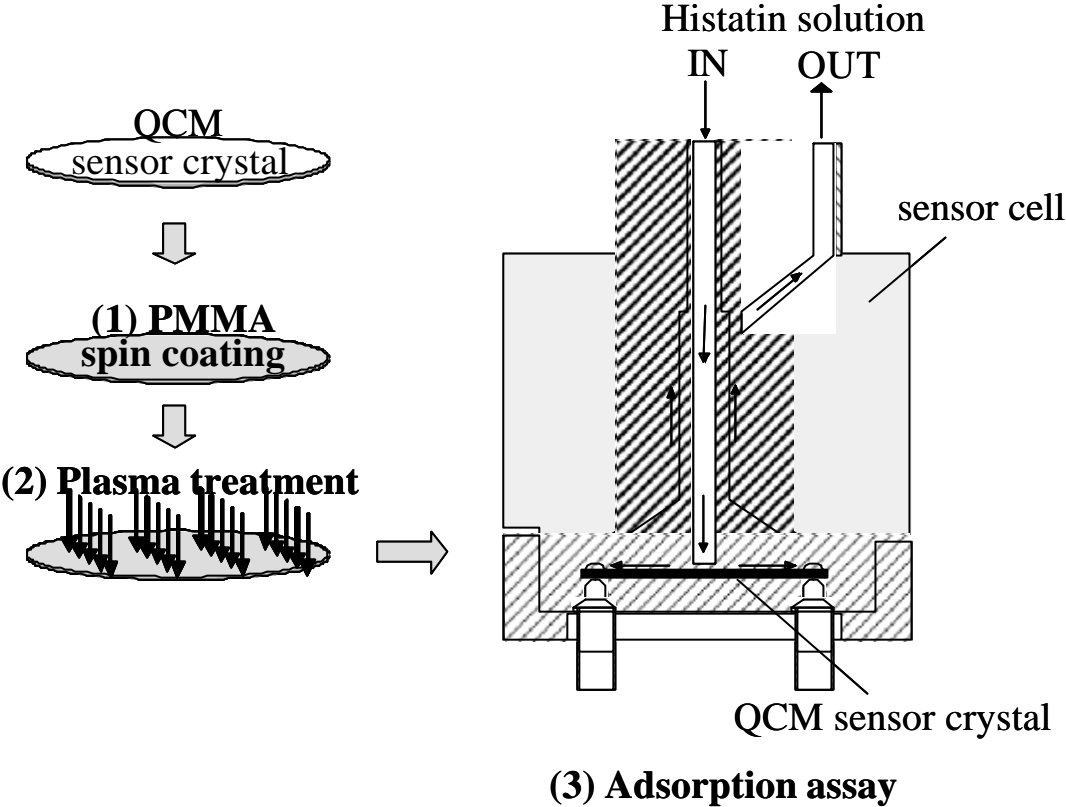


Figure 2 XPS spectra of PMMA and PMMA-O2 specimens.

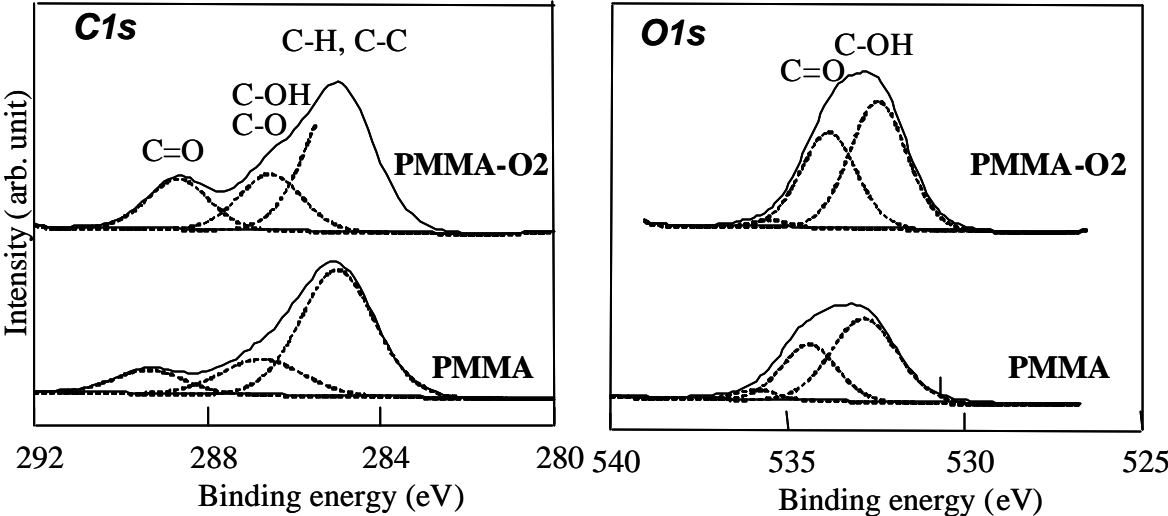


Figure 3 The intensity ratio of O /C element and carboxyl group to CHx group (C=O / C-H) on PMMA and PMMA-O2 surfaces. Identical letters indicate no significant difference ($p>0.05$).

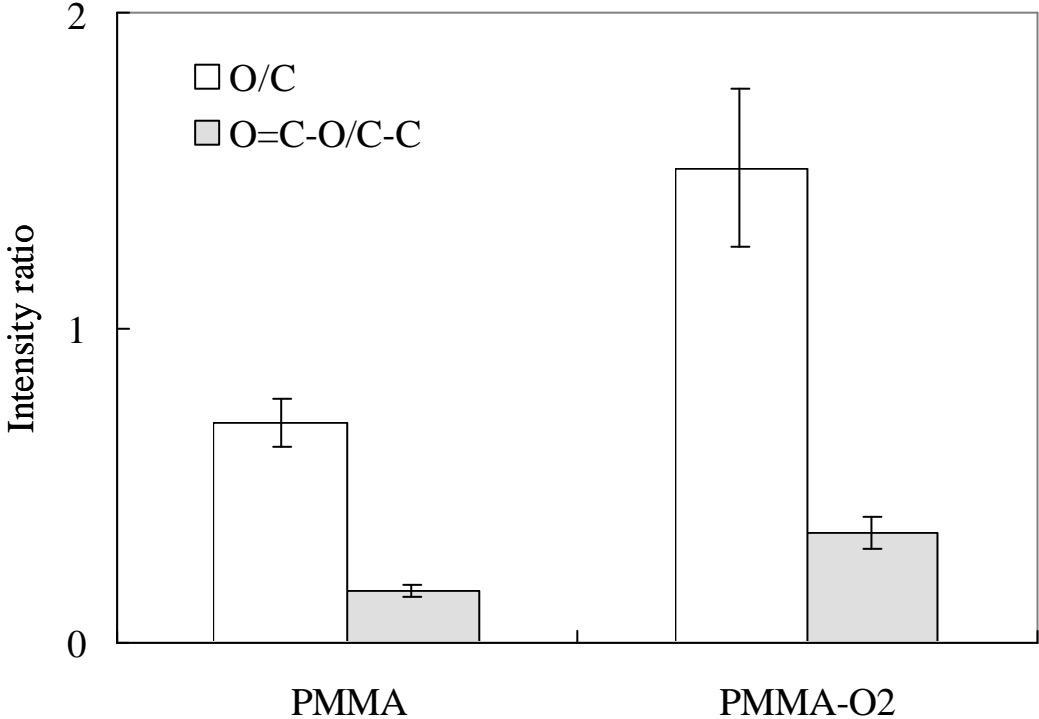


Figure 4 FT-IR spectra of the PMMA and PMMA-O2 specimens.

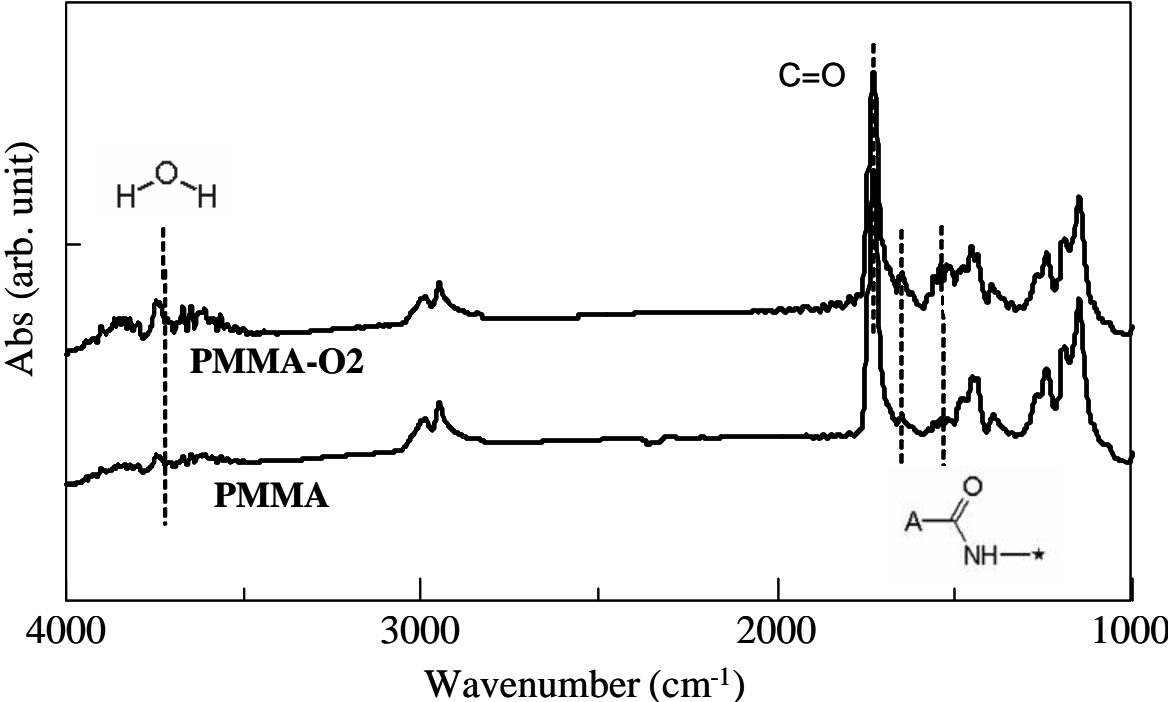


Figure5 (a) Δf and ΔD versus time, and (b) the ΔD - Δf plot of histatin-5 adsorption on PMMA-O2 specimen as a schematic example.

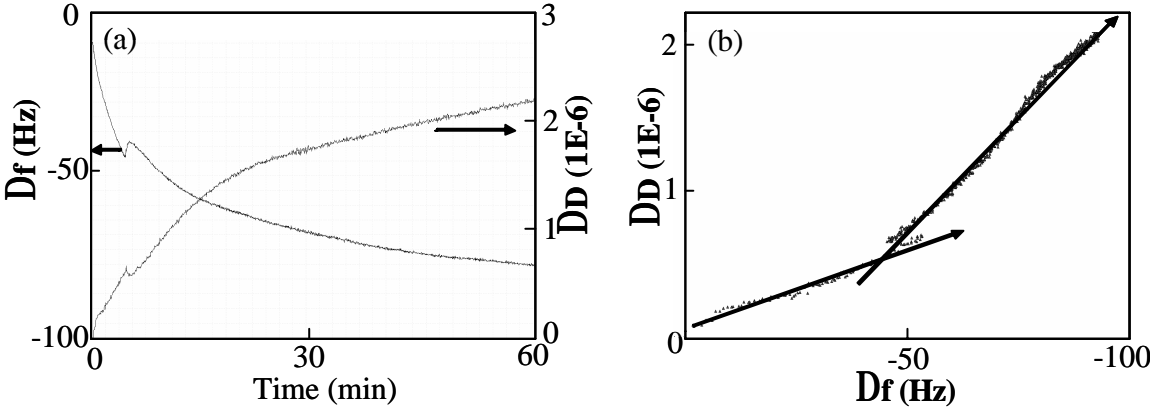
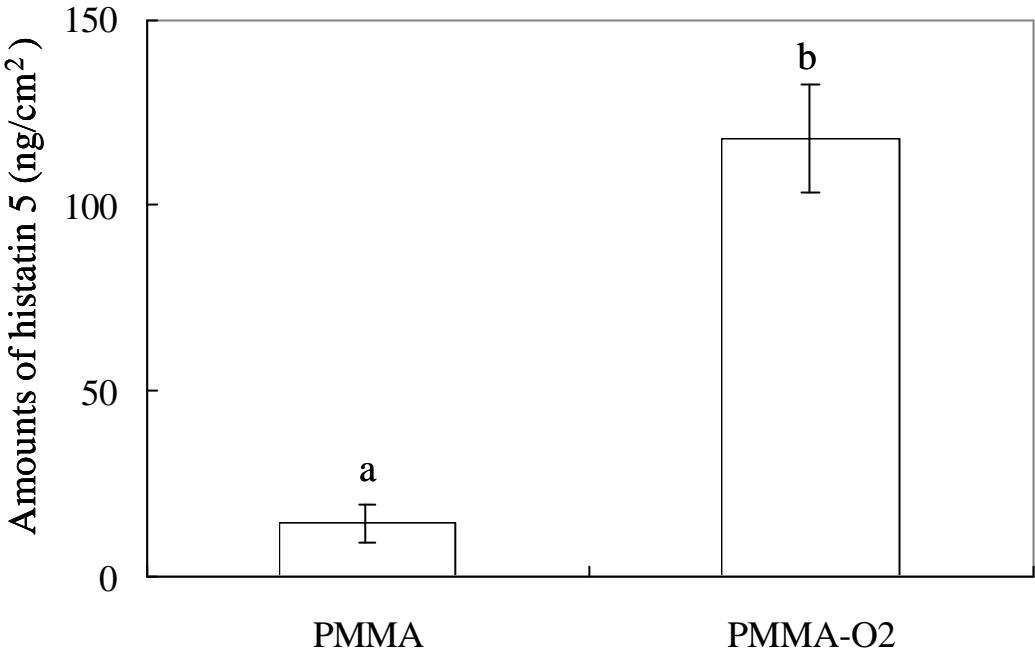


Figure 6 Estimated amounts of histatin 5 adsorption on QCM sensors. The contact angle and zeta-potential are also shown in this figure. Identical letters indicate no significant difference ($p>0.05$).



Contact angle(°)	68±4 ^a	14 ± 2 ^b
zeta-potential (mV)	-38 ± 5 ^{a'}	-28 ± 7 ^{a'}

Figure 7 (a) Typical example of shift in frequency and dissipation against time for exposure of PMMA specimen to *C. albicans*. The SEM images are also shown in (a).

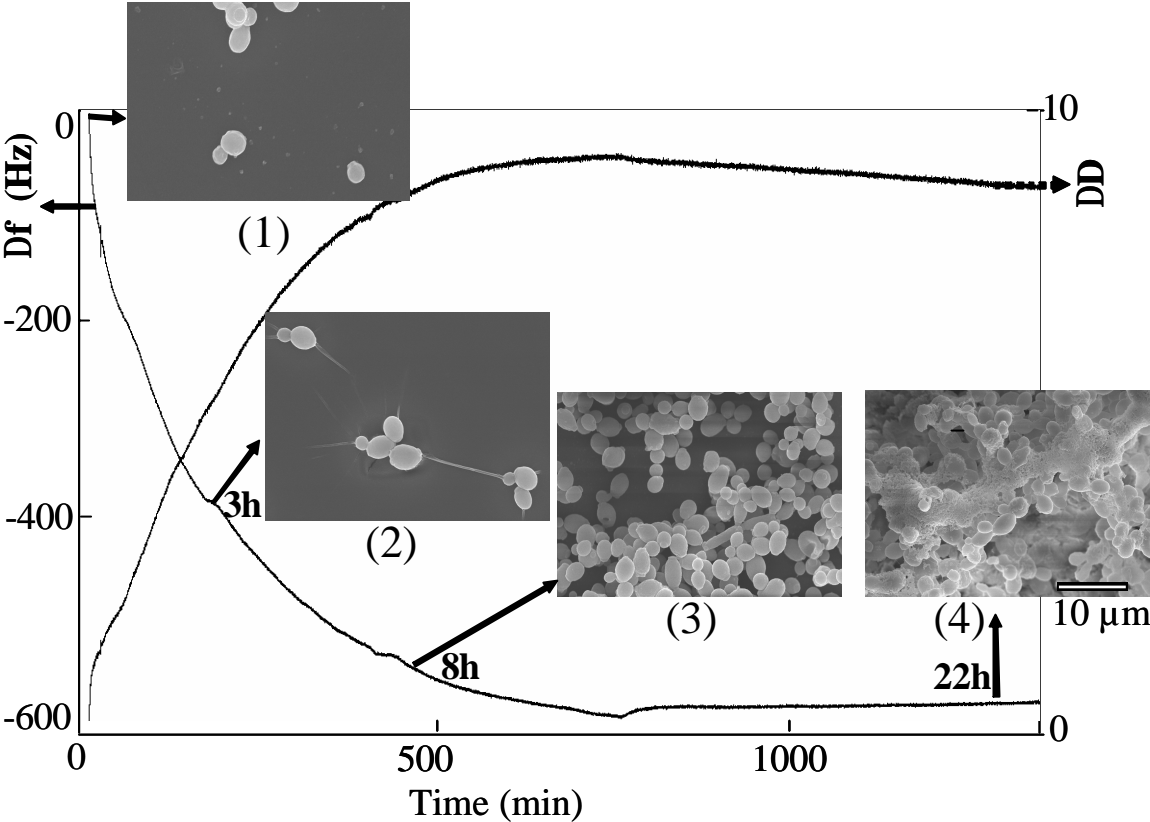


Figure 7 (b) ΔD - Δf plot of (a) as a schematic example.

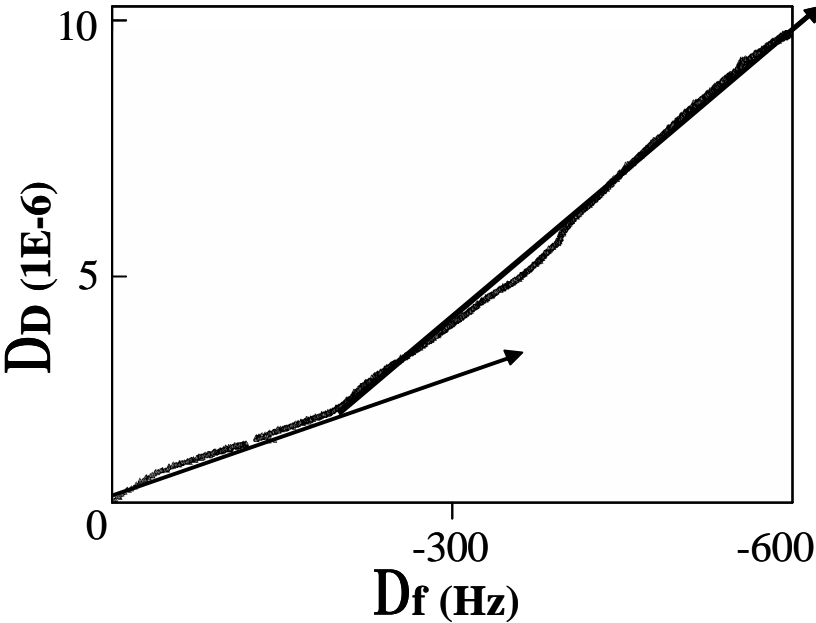


Figure 8 Amounts of *C. albicans* initially attached and colonized. Identical letters indicate no significant difference ($p > 0.05$).

